Behavior of High-Strength Friction-Grip Bolted Shear Connectors in Sustainable Composite Beams

Xinpei Liu[1]; Mark A. Bradford, Dist.M.ASCE[2]; and Michael S. S. Lee[3]

Abstract: Composite beams comprised of concrete slabs and steel beams joined by mechanical shear connectors are commonly used in modern building design. The use of innovative deconstructable high-strength friction-grip bolt (HSFGB) shear connectors and reduced-emissions precast geopolymer concrete slabs in composite beam design can greatly enhance the sustainability of building infrastructure. Hitherto, research contributions that address the behavior of composite beams with HSFGB shear connectors and precast geopolymer concrete slabs are very limited. To provide a contribution to this area of research, an effective finite element model of push-out testing is developed to investigate the ultimate strength and the load-slip characteristics of shear connection using HSFGB connectors and geopolymer concrete slabs in this proposed sustainable composite beam application. The accuracy of the proposed finite element model is validated by comparing its predictions with experimental results on push-out test specimens also reported in the paper. The effects of the change in the bolt pretension, its clearance between the hole in the steel flange, its diameter and tensile strength,and the compressive strength of the geopolymer concrete are elucidated through parametric studies. Practical design recommendations in algebraic form are proposed and verified for predicting the ultimate strengths and the load-slip relationships for composite beams with HSFGB shear connectors. **DOI: 10.1061/(ASCE)ST.1943-541X.0001090.**

Author keywords: Composite beams; Friction-grip bolt; Geopolymer concrete; Push-out test; Finite element model; Sustainable construction; Metal and composite structures.

Introduction

Structural composite steel–concrete beams are produced by connecting a concrete slab to its supporting structural steel beam using mechanical shear connectors. In the evolution of this technology, composite beams were considered initially as being very favorable for highway bridge construction because they could be erected rapidly and were very efficient structurally. More recently and because of the advent of profiled steel decking, composite steel and concrete flooring systems have been employed extensively in modern steel-framed buildings. Mechanical shear connectors are used to ensure robust composite action in composite steel-concrete beams, which require the transfer of shear forces at the interface of the supporting steel beam and slab. There are many types of mechanical shear connectors (as in the textbooks of Oehlers and Bradford 1995; Viest et al. 1997; Johnson 2004), but the most widely used ones are the headed stud shear connectors shown in Fig. 1(a), because they can be installed by rapid welding procedures and because they provide robust and ductile shear connection. However, contemporary issues related to deconstructability and the recycling of building infrastructure at the end of its service life are becoming increasingly important from the viewpoint of sustainable development (e.g., Vanegas 2004; Institution of Structural Engineers 2012; National Sustainability Council 2013), and it is self-evident that conventional composite beams with headed stud shear connectors cast into the concrete slab are unable to be decommissioned easily and efficiently during deconstruction or building modification. Accordingly, high-strength friction-grip bolt (HSFGB) shear connectors as shown in Fig. 1(b), which can be unbolted to deconstruct the building or to alter part of it structurally, can be used to replace headed stud shear connectors in composite beams. Despite this, studies of the behavior of HSFGB shear connectors in composite steel–concrete beams in the open literature are quite limited. Marshall et al. (1971) undertook an experimental study using the HSFGBs as shear connectors in composite steel-concrete beams, but the motivation for this work is unclear. Dallam (1968) and Dallam and Harpster (1968) undertook comprehensive tests on bolted shear connectors for the Missouri Highways Department, but the bolts were embedded in the concrete slab. Recently, three types of post-installed shear connectors were tested by Kwon et al. (2010) under static and fatigue loading for investigating methods to develop composite action in existing noncomposite bridges, whereas Pavlovic et al. (2013) have reported on the use of bolts with prefabricated composite decks.

Ordinary portland cement (OPC) has been used as a paste to produce concrete for a great many decades. As the most utilized construction material, OPC-concrete consumes significant amounts of natural resources during its manufacture and emits large amounts of CO_2 (Davidovits et al. 1990), which is known to contribute significantly to global warming (McCaffrey 2002). Several efforts are in progress to minimize the use of OPC-concrete in building construction to address the global warming issues. Geopolymer concretes (GPCs), that utilize industrial aluminosilicate waste materials such as fly ash and blast furnace slag as the binder, are an ideal

[1]Research Associate, Centre for Infrastructure Engineering and Safety, School of Civil and Environmental Engineering, Univ. of New South Wales, Sydney, NSW 2052, Australia.

[2]Scientia Professor and Australian Laureate Fellow, Centre for Infrastructure Engineering and Safety, School of Civil and Environmental Engineering, Univ. of New South Wales, Sydney, NSW 2052, Australia (corresponding author). E-mail: m.bradford@unsw.edu.au

[3]Ph.D. Student, Centre for Infrastructure Engineering and Safety, School of Civil and Environmental Engineering, Univ. of New South Wales, Sydney, NSW 2052, Australia.

Note. This manuscript was submitted on September 2, 2013; approved on March 20, 2014; published online on July 24, 2014. Discussion period open until December 24, 2014; separate discussions must be submitted for individual papers. This paper is part of the ***Journal of Structural Engineering***, © ASCE, ISSN 0733-9445/04014149(12)/$25.00.

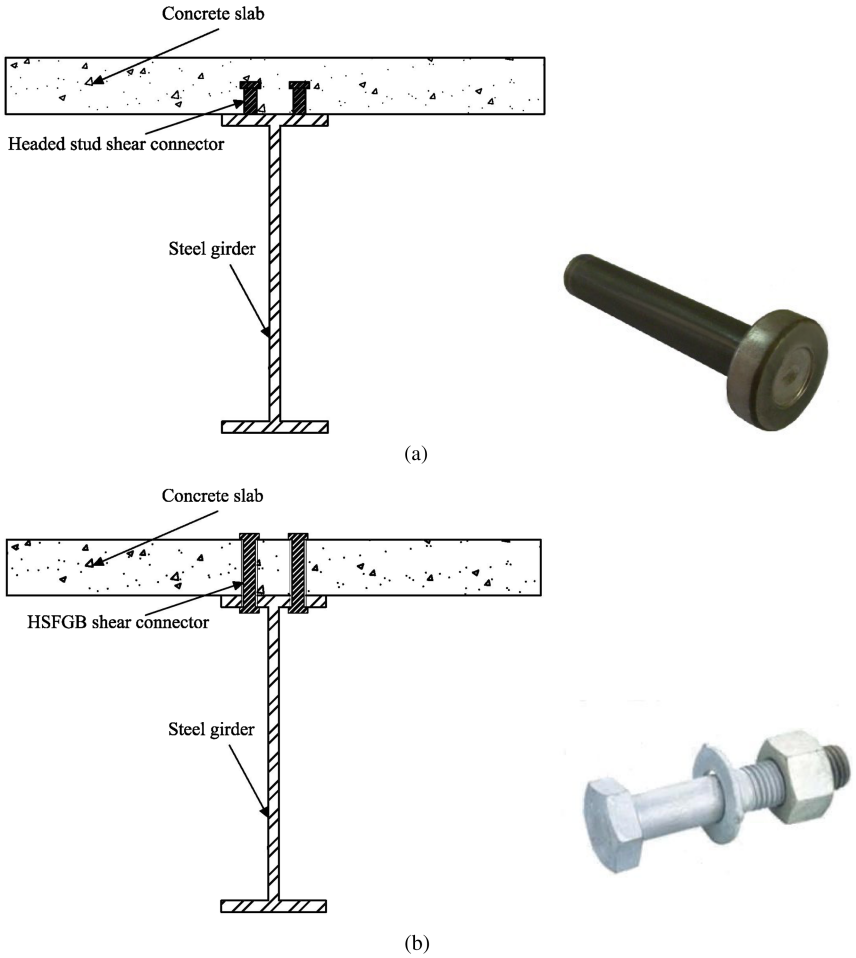

Fig. 1. Cross sections of composite beams with different shear connectors: (a) headed stud shear connectors; (b) HSFGB shear connectors

replacement for traditional OPC-concretes (Ng and Foster 2008). These concretes not only have a lower greenhouse footprint, but they also have excellent compressive strength, superior durability as well as small shrinkage deformations, and are suitable for structural applications (Rangan 2009). However, GPC is not readily batched on-site or is as workable by comparison to OPC-concrete, and so its use in precast applications is an important research issue. With the use of HSFGB shear connectors, precast GPC slabs have potential application to a composite structural system with the attributes of deconstructability and low CO_2 concrete slabs that contribute to sustainable development and construction.

The behavior of HSFGB shear connectors in composite beams with precast GPC slabs has been investigated experimentally from push-out tests (Lee and Bradford 2013a, b). Although the push-out tests provided a clear insight to the behavior of these connectors, the tests are costly and time consuming. Therefore, the main objective of this paper is to develop an accurate and efficient three-dimensional (3D) finite element (FE) model to investigate the behavior of HSFGB shear connectors in composite beams with precast GPC slabs, by modeling push-out tests initially. Because *ABAQUS* software is deployed, geometric and material nonlinearity are taken into account by default in the model. The results obtained from the FE analysis are verified against the experimental results from the push-out tests conducted as part of the research program. Extensive parametric studies are then performed to investigate the effects of the variations in the bolt pretension, the clearance between the hole and the bolt, the diameter and tensile strength of the bolt connector and compressive strength of the GPC. A practical design recommendation for the shear connection capacites and an algebraic load-slip curve for HSFGB shear connectors are also proposed in the paper.

Description of Push-Out Test Specimens

Fig. 2 shows the arrangement of the push tests used to determine the shear resistances and the load-slip behavior of HSFGB shear connectors in composite beams with precast GPC slabs. The push test specimens consist of an Australian 360 UB 56.7 steel beam (SA 1996) and two concrete slabs that are 450-mm long, 500-mm wide and 100-mm thick attached to the flanges of the steel beam. At the bottom of the specimen, the concrete slabs recess 50 mm into the steel beam to accommodate for the interface slip during testing. Square SL102 reinforcement mesh (having 9.5- mm diameter wire and 200-mm pitch) were cast in the concrete slabs in two layers to limit the splitting of the slabs. Two types of high strength structural bolts, M20 8.8 bolts and M16 8.8 bolts, were installed through prefabricated holes in the concrete slabs and the steel beam flanges to assemble the specimen by applying bolt pretension. The bolt pretension was applied by using an electric torque-control wrench and direct tension indicating washers were used to confirm the applied pretension. To eliminate any horizontal resistance being imposed by the slabs, a roller support was inserted at one end of the specimen. The test load was applied vertically on the upper part of the steel beam by a hydraulic jack. The slip between the steel beam and

(a)

(b)

Fig. 2. Arrangement of push-out tests: (a) preparation of test specimen; (b) experimental set-up

the concrete slabs was measured using linear variable displacement transducers (LVDTs). Details of the geometry of the push test specimens are shown in Fig. 3.

Finite Element Model

In this study, the FE program *ABAQUS* was used to simulate the push tests. To obtain accurate results from the FE analysis, all components influencing the behavior of the shear connection were properly modeled. The pertinent components are the concrete slabs, steel beams, HSFGB shear connectors with washers and the steel reinforcement. Both geometric and material nonlinearities were taken into consideration in the FE analysis.

Finite Element Mesh

Because of the symmetry of the specimens, only one quarter of the push test arrangement was modeled, with combinations of 3D solid elements being used to model these specimens. For both the concrete slabs and the structural steel beams, a 3D eight node element (C3D8R in *ABAQUS*) was used, which also improves the rate of convergence. A 3D twenty node quadratic brick element (C3D20R in *ABAQUS*) was chosen for the bolt shear connectors because of its ability to capture stress concentrations more efficiently as well as for its favorable geometric modeling features. A two node linear 3D truss element (T3D2 in *ABAQUS*) was adopted for the steel reinforcement. To reduce the computation time, a coarse mesh was used for the overall member, with a fine mesh being adopted for the bolt shear connectors and for the region around the shear connectors to achieve accurate results. The approximate overall mesh scale was 20 mm, with the smallest mesh scale being about 3 mm. The FE mesh of the push test model is depicted in Fig. 4.

Interaction and Constraint Conditions

Once all components of the FE model were properly positioned configured into the assembly, appropriate interaction and constraint conditions were defined among the various components. The surface-to-surface contact interaction available in *ABAQUS* was applied at all of the interfaces in the model, by specifying a hard contact property in the direction normal to the interface plane and the PENALTY option being used for the tangential behavior. The penalty frictional formulation with a friction coefficient equal to 0.45 (Lee and Bradford 2013a, b) was used for the contact interaction between the steel and concrete components, while the friction coefficient was taken as 0.25 for all of the other interactions. The embedded constraint was applied between the reinforcement and the concrete slab, so that the bars were embedded inside the slab by constraining the translational degrees of freedom of the nodes on the bar elements to the interpolated values of the corresponding degrees of the freedom of the concrete elements. The effects of the relative slip and debonding of the reinforcement with respect to the concrete slabs were ignored.

Boundary Conditions

For the application of the boundary conditions as shown in Fig. 5, all nodes of the concrete slab in the opposite direction of loading (surface 1) were restricted from moving in the Y direction to resist the compression load. All nodes along the middle of the steel beam web (surface 2) were restrained from translating in the Z direction and rotating in the X and Y directions because of symmetry. All nodes of the steel beam flange and concrete slab that lie on the other symmetry surface (surface 3) were prevented from translating in the X direction and rotating in the Y and Z directions.

Load Application and Analysis Steps

The uniformly distributed test load was applied as an imposed downward displacement of the top (cross-sectional) surface of steel beam as shown in Fig. 5. The analysis consisted of several steps. In the first step, the contact interactions were established to ensure that numerical problems resulting from the contact formulation will not be encountered during the following steps. The pretensioning forces were applied during the second step of the analysis by using the BOLT LOAD function available in *ABAQUS*. It should be noted that in usual practice the diameter of a predrilled hole is between 2 and 4 mm larger than the diameter d_b of a bolt. In this case, the magnitude of the bolt load should be the same as that of the applied bolt pretension. However, for an oversize hole that is 4 mm larger than d_b but not exceeding $1.25d_b$ or $(d_b + 8)$ mm in diameter (whichever is the greater), the magnitude of the bolt load should be reduced by a factor that allows for the shape and size of the hole in relation to the bolt (SA 1998), which was taken as 0.5 herein. In the subsequent step, the initial adjustment of the pretension section was maintained by using the *fix at current length* method in *ABAQUS*. This technique enables the load across the pretension section to change according to the externally applied loads to maintain equilibrium. If the initial adjustment of a section is not

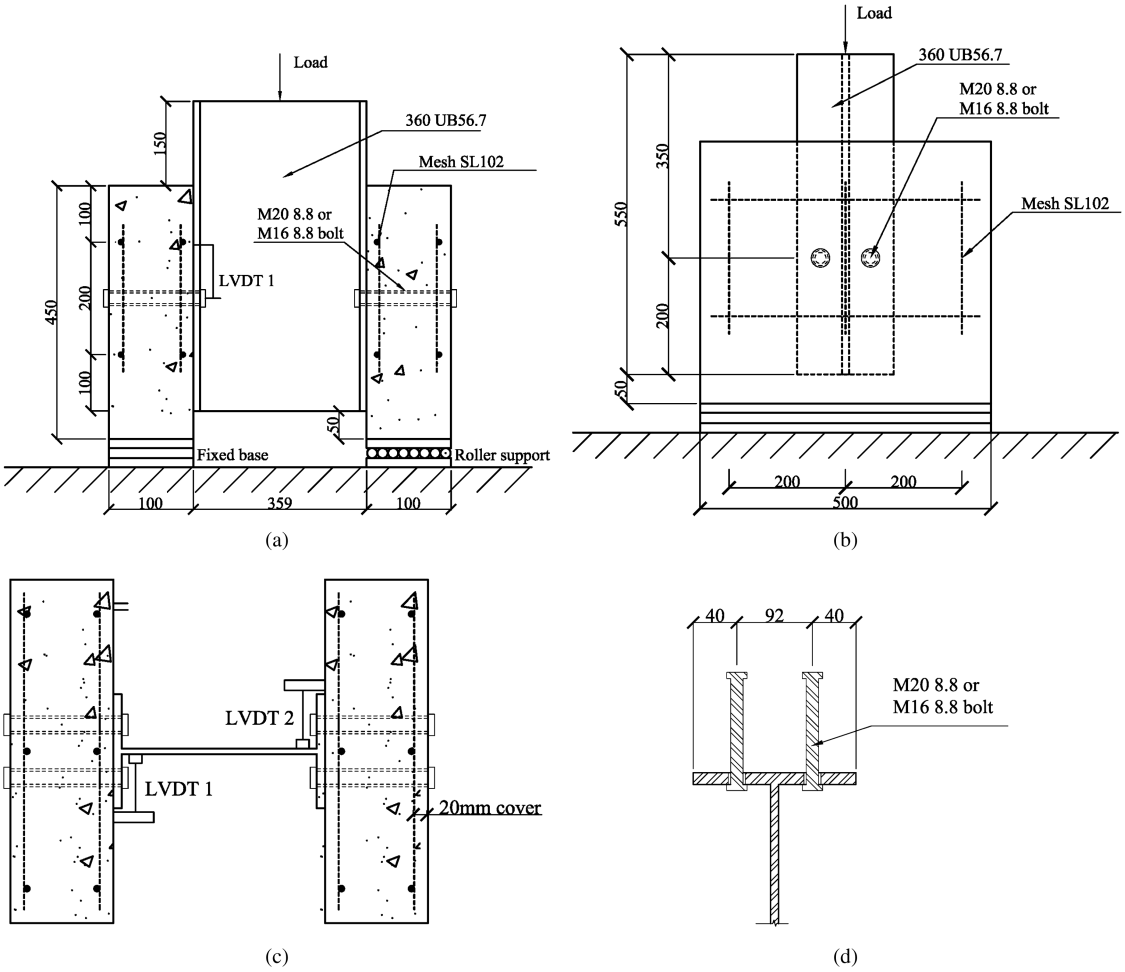

Fig. 3. Details of push-out test specimens: (a) front elevation view; (b) side elevation view; (c) plan view; (d) details of shear connectors

maintained, the force in the bolt will remain constant. Lastly, displacement-controlled nonlinear analysis was performed by using the RIKS method in *ABAQUS*, which is generally used to predict the unstable and nonlinear collapse of a structure. It is based on the arc-length control procedure that is invoked to trace the nonlinear load-deformation path. The initial increment can be adjusted if the FE model fails to converge. Subsequently, the value of load after each increment was computed automatically. The final result was either the maximum value of the load or the maximum value of the displacement. To identify the bolt fracture failure in the push-out test, the strains in the bolts were monitored during the analysis. Most of the strains in the weakest cross-section of the shank approached the expected fracture limit value, indicating bolt shear connector fracture.

Material Model for Concrete Slab

For structural computations with GPC, little research is available in the open literature and so some assumptions are needed (Bradford and Pi 2012a, b), these being essentially derived from the computational modeling of normal concretes. The nonlinear behavior of the GPC concrete material in the push-out tests was represented by an equivalent uniaxial stress-strain curve as shown in Fig. 6(a). Three parts of the idealized curve can be identified. The first part is assumed to be in the elastic range initially, up to the limit of proportionality stress. As suggested by Nguyen and Kim (2009), the value of this stress is taken as $0.4f_{ck}$, where f_{ck} = compressive cylinder strength of the concrete, which is equal to $0.8f_{cu}$, where f_{cu} = compressive cube strength of the concrete. The Australian Standard AS3600 (2009) recommends that the elastic modulus of OPC-concrete be taken as

$$E_c = \rho^{1.5}(0.024\sqrt{f_{\text{cm}}} + 0.12)\ \text{(MPa)} \tag{1}$$

where ρ = density of the concrete in kg/m^3 and f_{cm} = mean compressive cylinder strength in MPa. For GPC, Rangan (2009) found that the elastic modulus is approximately 25% lower than that of OPC, so a value of $0.75E_c$ was used for the GPC. The Poisson's ratio was taken as 0.2. The second part of the curve is the nonlinear parabolic portion starting from the proportional limit stress $0.4f_{ck}$ to the peak stress f_{ck}. This part of the curve can be determined from the equation

$$\sigma_c = f_{ck}\left(\frac{\varepsilon_c}{\varepsilon_{ck}}\right)\left[\frac{n}{n-1+(\varepsilon_c/\varepsilon_{ck})^{nk}}\right] \tag{2}$$

where ε_{ck} = strain at the peak stress, $n = 0.8 + f_{ck}/17$, and $k = 0.67 + f_{ck}/62$ when $\varepsilon_c/\varepsilon_{ck} > 1$ or $k = 1$ when $\varepsilon_c/\varepsilon_{ck} \le 1$. This equation was firstly proposed by Collins et al. (1993) to predict the stress-strain relationship for OPC-concrete in compression, and its use was recommended by Hardjito and Rangan (2005) for GPC as well. The strain at the peak stress is assumed to be 0.002 for OPC concrete and 0.0033 for GPC based on empirical data. The third part of the curve is the constant without a decrease

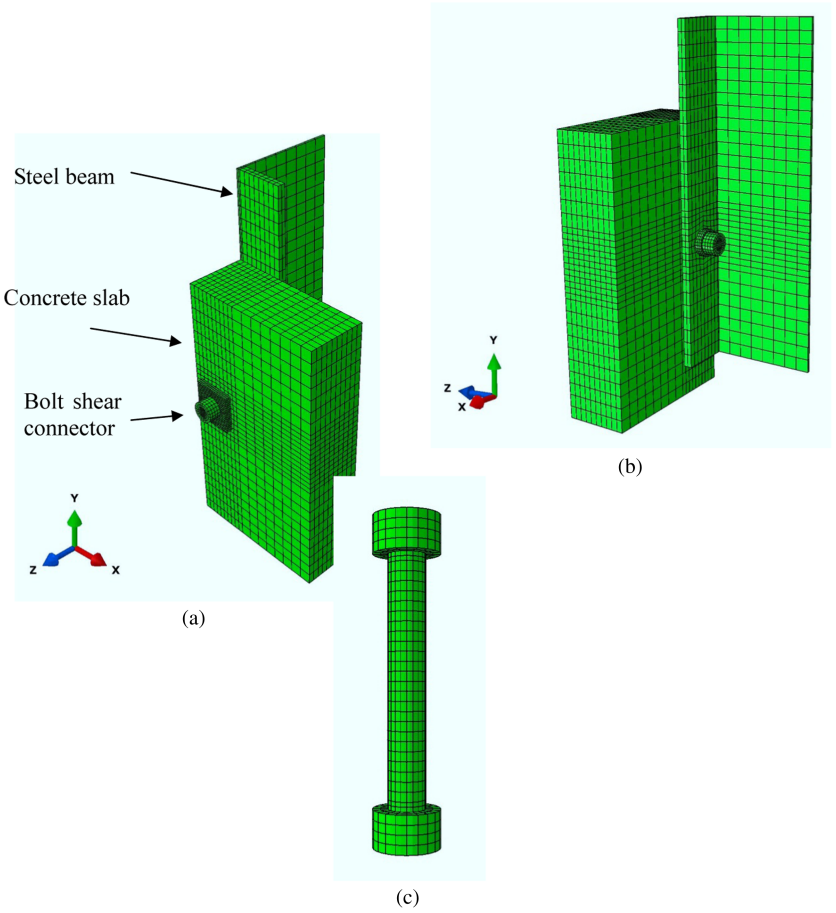

Fig. 4. Finite element mesh of model: (a) 3D view 1; (b) 3D view 2; (c) bolt shear connector

of stress after the peak compressive strength is reached. This perfect plastic behavior is assumed for the modeling, since the benign behavior of the concrete in compression has been observed in composite beam tests (Nguyen and Kim 2009). This behavior is probably because the concrete is confined in a triaxial stress state in the regions around the shear connectors, which would be expected to be more profound with HSFGB shear connectors because of the tension in the bolts. The PLASTIC model available in *ABAQUS* was used to specify the plastic part of the concrete material model that uses a von Mises yield surface (Ellobody and Lam 2002; Lam and Ellobody 2005). It was assumed that the tensile splitting of the concrete slab was prevented. Of course, this simplifying assumption precludes the consideration of tensile stresses in the concrete greater than its tensile strength around $0.4\sqrt{f_{ck}}$.

Material Model for Steel Beam, Reinforcement, and HSGFB Shear Connectors

For the steel beam, its effect is insignificant on the overall performance of a push-out test, whose main function is to allow for the transmission of the applied loads to the connectors. The stress-strain response of the steel beam was represented by the bilinear relationship shown in Fig. 6(b). The stress-strain curves for the reinforcement and HSFGB shear connectors, as measured by Loh et al. (2006), were also simulated as having a bilinear stress-strain model. They behave as linear elastic materials with a modulus of elasticity E_s up to the yield stress f_{ys}, followed by fully plastic behavior, but with the HSFGB response being limited by a fracture strain of 0.15 (Shi et al. 2008). The modulus of elasticity for the steel beam, reinforcement and HSGFB shear connectors was taken as 200 GPa, with respective yield stresses of 390, 500, and 1020 MPa.

Results and Discussion

As part of the present study, experimental push-out tests were undertaken to evaluate the accuracy of the FE modeling. Five

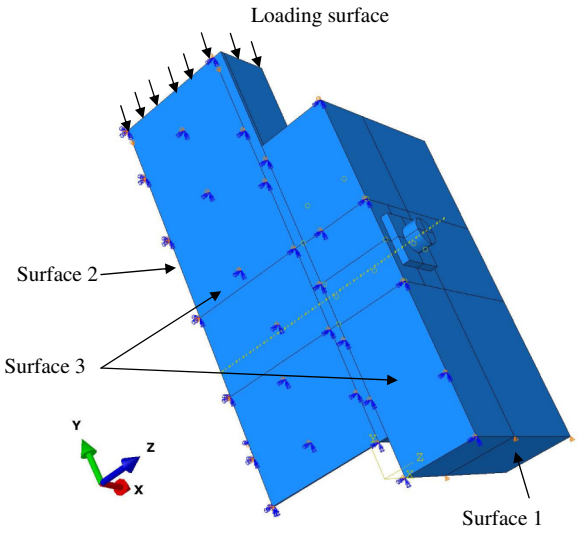

Fig. 5. Boundary conditions and loading surfaces

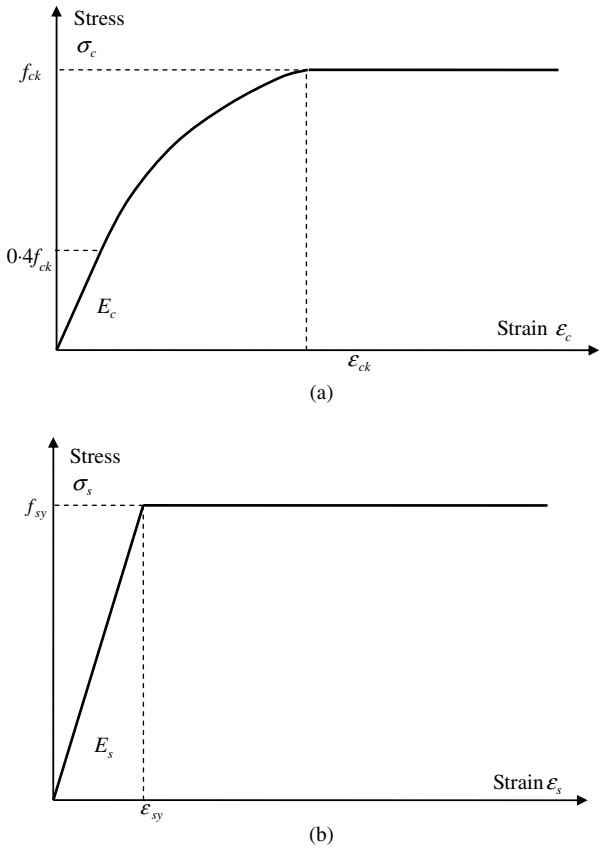

Fig. 6. Stress-strain relationships: (a) GPC material; (b) steel beam, reinforcement and HSGFB shear connector

specimens with different pretension forces, diameters of the holes in the slabs and diameters of the bolts were tested; the diameter of the hole in the steel flange was 24 mm for each. The testing procedure was carried out according to Eurocode 4 [British Standards Institution (2004)], with each specimen being loaded initially to 40% of the expected failure load, and then cycled 25 times between 5 and 40% of the expected failure load. Following this, each specimen was loaded monotonically under displacement control until failure. The material properties of the GPC were determined in accordance with AS 1012 (SA 1997, 1999). The average compressive cylinder strength of the GPC on the day of testing was measured as 47 MPa, and its modulus of elasticity was measured as 23 GPa. (The density ρ was not measured, but by comparison Eq. (1) with $\rho = 2{,}400$ kg/m^3 produces $0.75E_c = 26$ GPa). Table 1 gives detailed information for the five push-out test specimens, and a comparison of the ultimate shear connection resistance per bolt obtained from the tests Q_{Test} and from the FE analysis Q_{FE}. The ultimate resistance of the shear connector is determined based on the obtained maximum load from the push-out test. There is good agreement between the experimental and numerical results for all of the push-out tests, with a maximum difference of 7% observed between both of the results for specimen SP3. The mean value of $Q_{\text{Test}}/Q_{\text{FE}}$ is 1.02 with the coefficient of variation (COV) being 4.7%. The experimental load-slip curves measured for the specimens are compared with the numerical curves obtained from the FE element analysis in Figs. 7(a–d). The load–slip response obtained from the FE analysis has close agreement with the experimental response.

For specimen SP1, 20-mm diameter bolts pretensioned with a 145 kN standard bolt load were used. The diameter of the hole in the slab is 24 mm for each. The load-slip response exhibited three distinct regimes. At the early stage of loading, the shear connection had a very high stiffness because the pretensioning of the HSFGB shear connectors induces mechanical friction between the slab and steel flange as being the mechanism of shear transfer. As can be seen, the slip at 50 kN of load is less than 0.1 mm. After the friction at the steel-concrete interface induced by the pretension in the shear connectors was overcome, significant slip occurred at the steel-concrete interface because effective installation of the shear connectors always requires significant clearance between the prefabricated holes and the bolts. The critical slip in test SP1 was approximately 4 mm, being close to the sum of the clearance between the hole in the steel beam flange and the bolt and the clearance between the hole in the concrete slab and the bolt. After the bolt commenced to bear against the surface of the hole in the slab, the HSFGB shear connectors showed similar load-slip characteristics to traditional headed stud shear connectors, except for a slightly lower initial stiffness. Specimen SP1 was not loaded to connector failure because of the significant cracking in both concrete slabs. Fig. 8 shows the stress contours and the deformed shape obtained from the FE model close to failure, from which it can be observed that the maximum stresses in the concrete are in the regions around the shear connectors in the form of a cone. However, unlike push-out tests with large headed stud shear connectors which have conical concrete failure modes as described by Lam and Ellobody (2005), the concrete in the regions of the shear connectors with pretensioned bolts has an additional confinement, and no conical concrete failures were observed in any of the push-out tests.

Specimen SP2 had the same dimensions and material properties as SP1. Firstly, it was loaded to 50 kN per bolt, which is in the expected range of serviceability loads at which slip is to be prevented to achieve close to full shear interaction. The specimen was then unloaded and the HSFGB shear connectors were unbolted as shown in Fig. 9, to illustrate the feasibility of the procedure for the deconstruction of the shear connection. The specimen was then reassembled and loaded until failure occurred, with the load-slip response being similar to that of SP1.

Specimen SP3 had smaller sized bolts (16 mm) pretensioned with a 95 kN standard bolt load, and oversized holes in the slabs.

Table 1. Comparison of the HSFGB Shear Connection Ultimate Resistances from Tests and FE Analysis

Specimen	Pretension (kN)	Slab hole diameter (mm)	Bolt diameter (mm)	Number of bolts	Number of slabs	Q_{Test} per bolt (kN)	Q_{FE} per bolt (kN)	$Q_{\text{Test}}/Q_{\text{FE}}$
SP1	145	24	20	4	2	216	214	1.01
SP2	145	24	20	4	2	223	214	1.04
SP3	95	24	16	4	2	153	143	1.07
SP4	70	28	20	4	2	202	214	0.94
SP5	145	28	20	8	4	216	214	1.01
			Mean					1.02
			Coefficient of variation					0.047

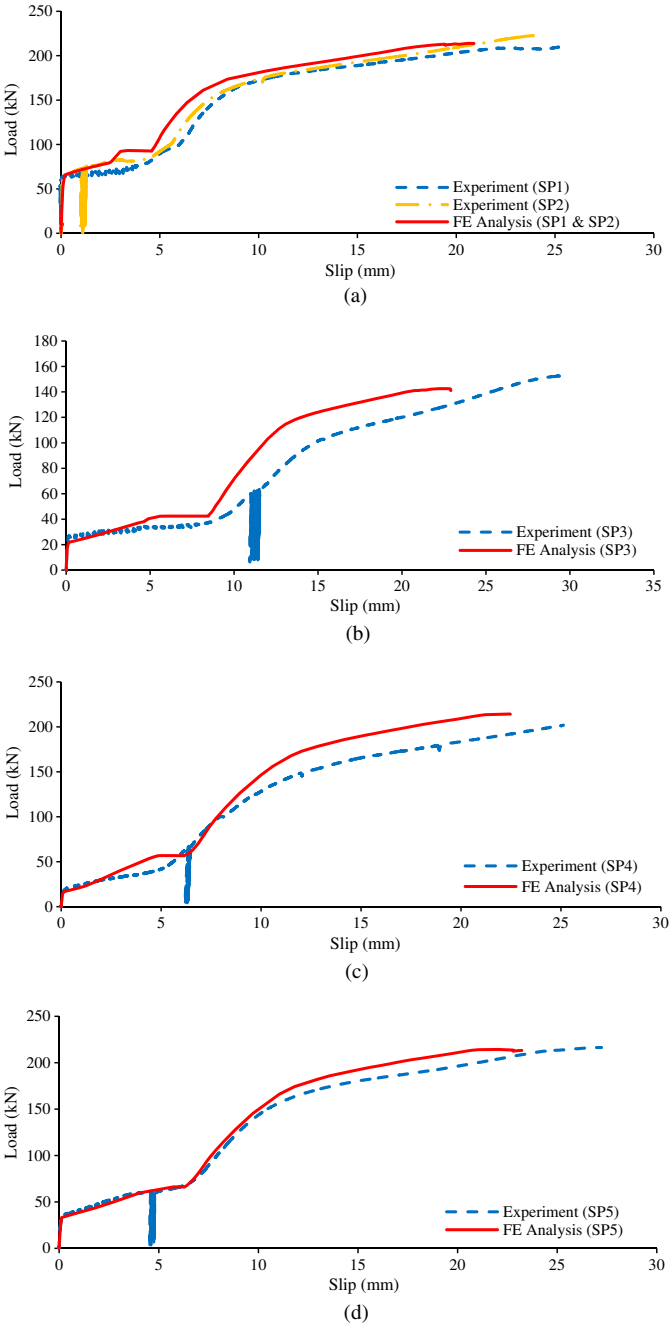

Fig. 7. Comparison of load-slip curves from tests and FE analysis: (a) SP1and SP2; (b) SP3; (c) SP4; (d) SP5

The first significant slip occurred at a load of 22.8 kN, compared with at 21.8 kN from the numerical analysis. The critical slip was about 6 mm. The specimen then failed by shear fracture of the bolt connector as shown in Fig. 10, with only a few small cracks being observed on the concrete surface after the test. On the other hand, 20-mm diameter bolts tightened with a smaller pretension of about 70 kN in oversized holes were used in specimen SP4. The first significant slip occurred at a load of 17.8 kN, compared with 16.7 kN from the numerical analysis, and the critical slip was also about 6 mm.

Test specimen SP5 as shown in Fig 2(b) was specially designed with the number of bolts and concrete slabs being increased two-fold, by stacking up two single slabs on each side of the push test specimen as would occur with the juxtaposition of precast GPC slabs in a real beam. Fig. 7(d) demonstrates that the load-slip curves obtained experimentally and numerically agree very well, the maximum experimental load being 216 kN per bolt at a slip of 26.8 mm compared with 214 kN at a slip of 23.6 mm obtained from the FE analysis. Based on its modeling of the push-out tests, the FE model developed in this study can successfully predict the ultimate shear resistances and load-slip response of shear connection that uses precast GPC slabs and HSFGB shear connectors, and because of this it is able to provide numerical modeling of the behavior of push-out tests and real composite beams.

Parametric Studies

Parametric studies have been carried out using the FE modeling of the push-out tests developed in this paper. The effects of variations in the bolt pretension, its clearance between the hole in the slab, its diameter and tensile strength and the compressive strength of the precast GPC slab on the shear connection resistances and load-slip behavior were investigated. The dimensions and material properties of the push-out specimens for the parametric studies are given in Table 2, and the corresponding ultimate shear connection resistances obtained from the FE analysis are summarized in Table 3.

Effect of Bolt Pretension and Diameter of Hole

Fig. 11 shows the load-slip relationships for the push-out test specimens in group G1. Different bolt pretensions, viz. 75, 100, 120, and 145 kN, were considered in this group. It is shown in Fig. 11 that by increasing the bolt pretension, the force needed to overcome the friction at the interface between the steel and the concrete leading to the first significant slip is increased. However, the change in the bolt pretension has no significant effect on the ultimate shear connection resistance. Fig. 12 shows the load-slip relationships for the push-out test specimens with different diameters of the prefabricated holes in group G2. The same 20-mm diameter bolts were installed in all of the three specimens, but different diameters for the holes, viz. 22, 24, and 28 mm, were chosen. As expected, the clearance between the prefabricated hole and the bolt directly affects the value of the first critical slip. In addition, specimen G2-3, with a significantly larger clearance hole, had not only a larger first critical slip, but it also required a smaller force to cause first slip, compared with specimens with the normal sized holes such as G2-1 and G2-2.

Effect of Diameter and Tensile Strength of Bolt Connector

The effects of the diameter and tensile strength of the bolt connectors on the load-slip response is illustrated in Figs. 13 and 14, respectively. The group of push-out specimens with bolt diameters of 16, 20, 22, and 24 mm is denoted as group G3 in Table 2, whereas the group of push-out specimens with tensile strengths of 830, 900, 1020, and 1,100 MPa is denoted as group G4 in Table 2. The figures show that both the load-slip relationship and the ultimate shear connection resistance are affected signficantly by changing either the diameter or the tensile strength of the bolt connectors. The shear connection stiffness, strength and ductility increase with an increase of either the diameter or the tensile strengths of the bolt shear connectors. For example, and as shown in Fig. 13, when the diameter of the bolt connectors is increased from 16 to 24 mm, the ultimate shear connection resistance increases by 113%, given that the tensile strengths of both bolts are 1,020 MPa. In addition, and as shown in Fig. 14, when the tensile strength of the 20-mm diameter bolt connectors increases from 830 to 1,100 MPa, the ultimate shear connection resistance increases by 34%.

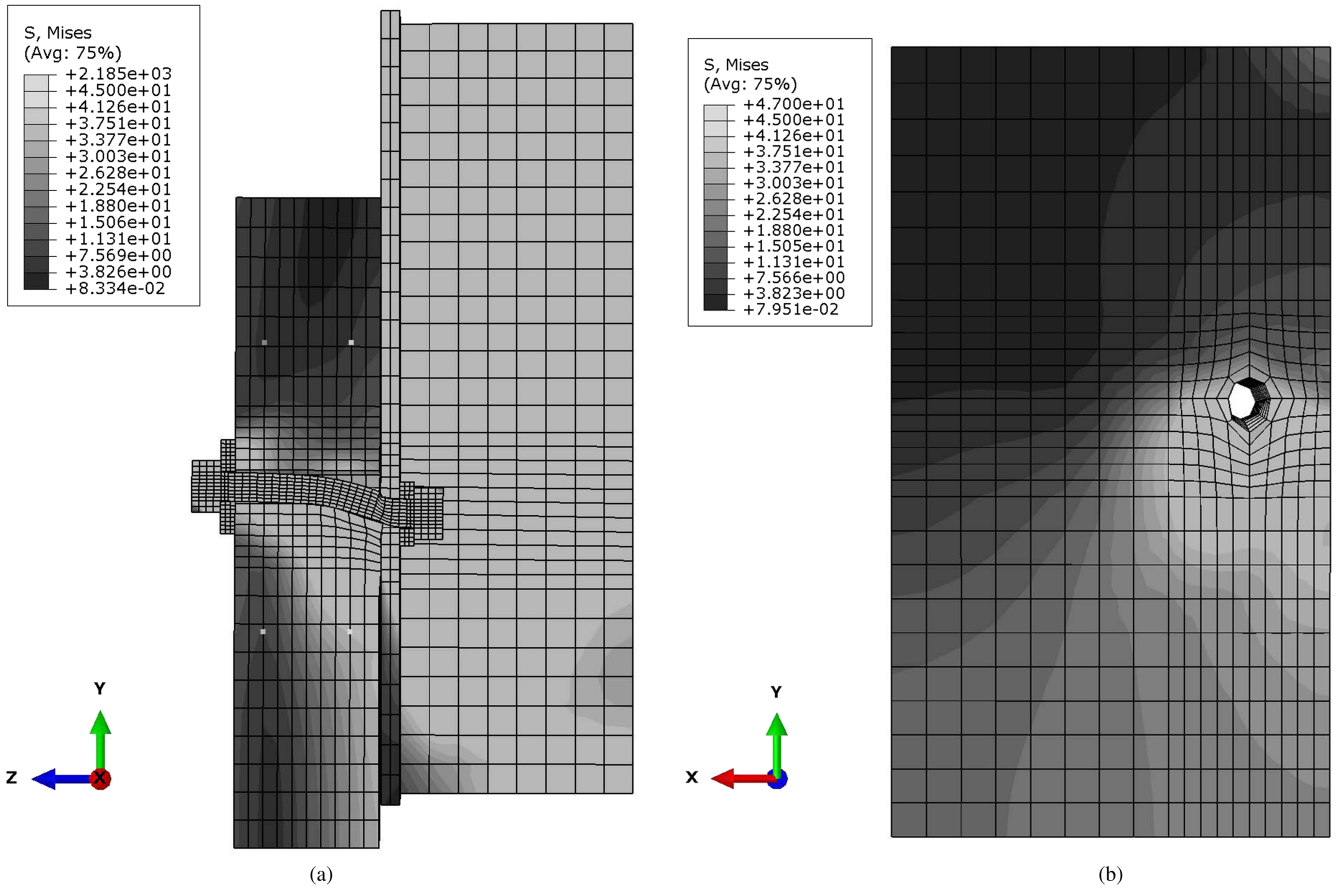

Fig. 8. Stress contours and deformed shape from FE model for specimen SP1: (a) cut view; (b) concrete slab

Effect of Strength of GPC Concrete

Fig. 15 shows the load-slip curves for the push-out specimens in group G5, having different compressive strengths of the GPC. The effect of the concrete compressive strength on the ultimate strength of the shear connection is negligible. This observation assumes that there is sufficient transverse reinforcement to ensure the tensile splitting of the concrete slab is prevented, because the tensile behavior of the slab is not modeled in the FE analysis. However, the change in concrete strength produces distinct influences on the load-slip behavior, because this is influenced by the elastic modulus of the concrete and so is influenced by the concrete compressive strength by virtue of Eq. (1).

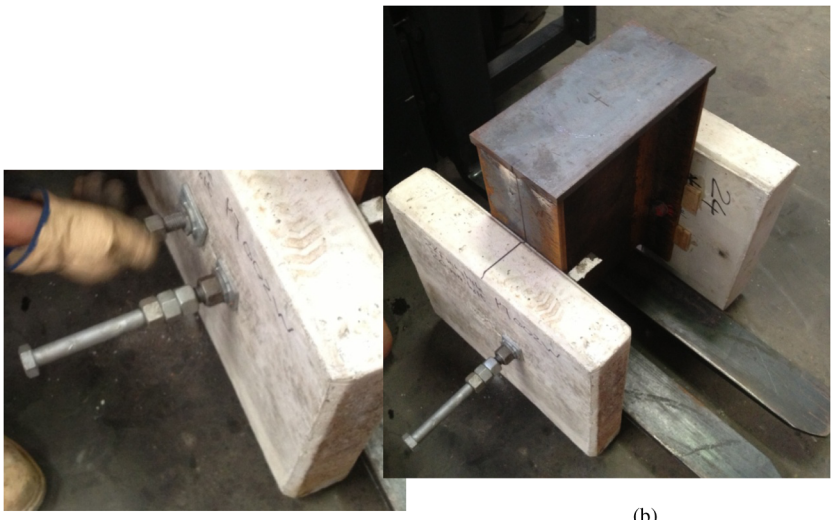

Fig. 9. Deconstructability of HSFGB shear connector: (a) unbolting; (b) unbolted

Design Recommendations

Kwon et al. (2010) proposed that the ultimate strength of postinstalled shear connectors Q_u under static loading is given by

$$Q_u = 0.5A_{sc}F_u \text{ (N)} \tag{3}$$

where A_{sc} = cross-sectional area of the bolt in mm^2 and F_u = tensile strength of the high strength bolt shear connector in MPa. To more accurately predict the ultimate strength of a HSFGB shear connector, the results from the present study suggest that Eq. (3) be modified to

$$Q_u = 0.66A_{sc}F_u \text{ (N)} \tag{4}$$

To propose equations to predict the load and slip displacement relationship of HSFGB shear connectors as shown in Fig. 16, the three distinct regimes of the load-slip response are taken into consideration. At the early stage of loading, the slip is almost zero because the connection uses friction as the means for shear transfer at the initial loading. Based on friction-grip bolt design methodologies (Trahair et al. 2008), the first significant slip occurs after the friction at the steel-concrete interface from the pretension of the shear connectors is overcome at shear force Q_0 that is given by

$$Q_0 = \mu_f k_h N_t \tag{5}$$

in which μ_f = coefficent of friction between the GPC slab and the steel beam and N_t = bolt tension. The factor k_h in Eq. (5) allows for the shape and size of the hole in relation to the bolt. Normally k_h is taken as 1.0. However, when either the diameter of the hole in the concrete slab d_c or in the steel beam flange d_s exceeds the diameter of the bolt d_b by more than 4 mm, k_h can be taken as 0.5. (The oversized hole should not exceed $1.25d_b$ or $(d_b + 8)$ mm in diameter, whichever is the greater). The critical slip in Δ_1 in Fig. 16 can be obtained from

Fig. 10. Shear fracture failure of bolt in specimen SP3

Table 3. Comparison of Shear Connection Ultimate Resistances from FE Analysis and Design Recommendation (DR)

Group	Specimen	Q_{FE} (kN)	Q_{Kown} (kN)	Q_{DR} (kN)	Q_{FE}/Q_{Kown}	Q_{FE}/Q_{DR}
G1	G1-1	212	160	211	1.32	1.00
	G1-2	212	160	211	1.33	1.00
	G1-3	211	160	211	1.32	1.00
	G1-4	214	160	211	1.33	1.01
G2	G2-1	212	160	211	1.32	1.00
	G2-2	214	160	211	1.33	1.01
	G2-3	213	160	211	1.33	1.01
G3	G3-1	141	103	135	1.38	1.04
	G3-2	212	160	211	1.33	1.00
	G3-3	255	194	256	1.31	0.99
	G3-4	301	231	305	1.31	0.99
G4	G4-1	173	130	172	1.33	1.00
	G4-2	186	141	187	1.32	1.00
	G4-3	214	160	211	1.33	1.01
	G4-4	232	173	228	1.34	1.02
G5	G5-1	214	160	211	1.34	1.01
	G5-2	212	160	211	1.32	1.00
	G5-3	212	160	211	1.32	1.00
	G5-4	211	160	211	1.32	1.00
Mean					1.33	1.01
Coefficient of variation					0.011	0.011

Table 2. Dimensions and Material Properties of the Push-Out Specimens for Parametric Studies

Group	Specimen	Pretension (kN)	Hole diameter (mm)	Bolt diameter (mm)	Tensile strength of bolt (MPa)	Compressive strength of concrete (MPa)
G1	G1-1	75	24	20	1,020	47
	G1-2	100	24	20	1,020	47
	G1-3	120	24	20	1,020	47
	G1-4	145	24	20	1,020	47
G2	G2-1	145	22	20	1,020	47
	G2-2	145	24	20	1,020	47
	G2-3	145	28	20	1,020	47
G3	G3-1	95	20	16	1,020	47
	G3-2	95	24	20	1,020	47
	G3-3	95	26	22	1,020	47
	G3-4	95	28	24	1,020	47
G4	G4-1	145	24	20	830	47
	G4-2	145	24	20	900	47
	G4-3	145	24	20	1,020	47
	G4-4	145	24	20	1,100	47
G5	G5-1	145	24	20	1,020	45
	G5-2	145	24	20	1,020	50
	G5-3	145	24	20	1,020	60
	G5-4	145	24	20	1,020	80

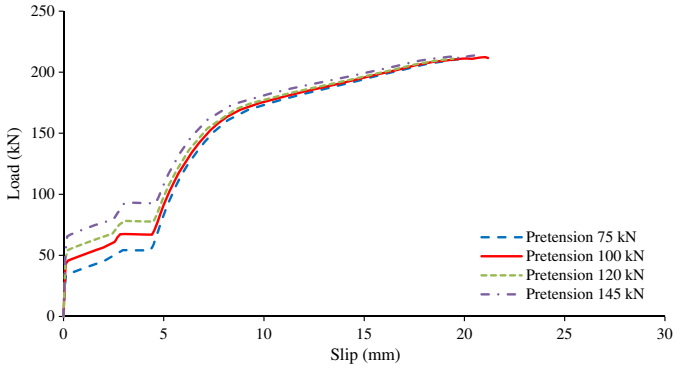

Fig. 11. Effect of the change in bolt pretension

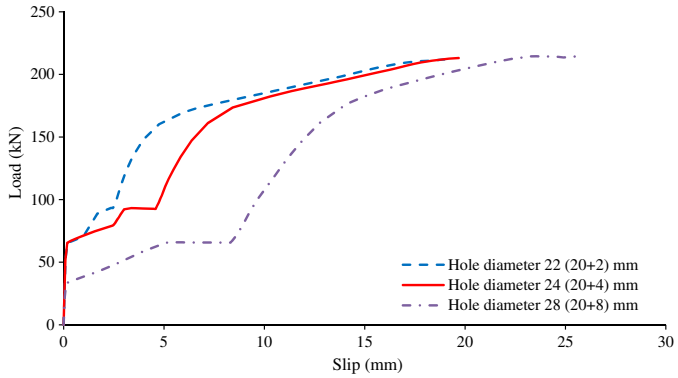

Fig. 12. Effect of the change in clearance between the hole and the bolt

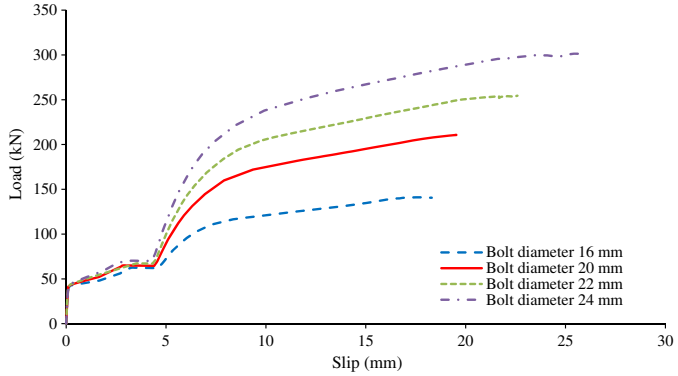

Fig. 13. Effect of the change in diameter of the bolt connector

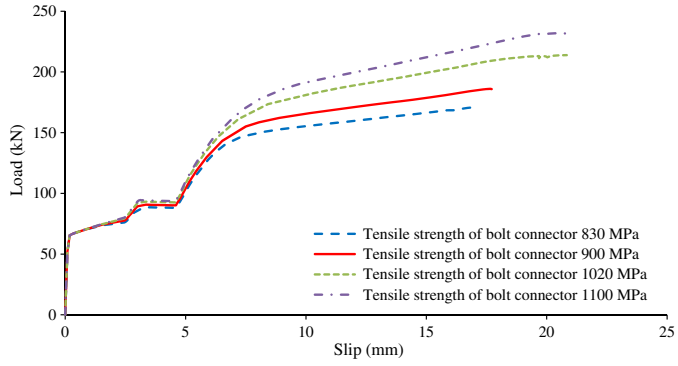

Fig. 14. Effect of the change in tensile strength of the bolt connector

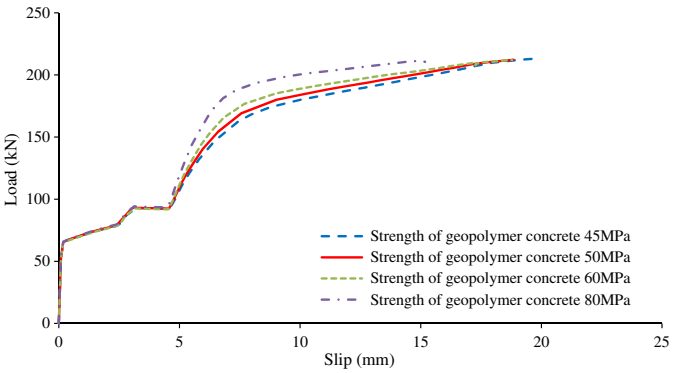

Fig. 15. Effect of the change in compressive strength of the geopolymer concrete

$$\Delta_1 = (d_c + d_s - 2d_b)/2 \tag{6}$$

for which the corresponding load in Fig. 16 is given by $Q_1 = Q_0 + 20\text{kN}$. After the bolt bears against the steel and concrete, the empirical formula for load-slip relationship of the shear connection is proposed as being

$$Q_{sh}(\Delta_{\text{slip}}) = Q_1 + (Q_u - Q_1)\{1 - \exp[-0.005 f_{ck}(\Delta_{\text{slip}} - \Delta_1)]\}^{0.8} \tag{7}$$

where Q_{sh} = applied shear force in shear connector (N), Δ_{slip} = slip of shear connector (mm) and f_{ck} = compressive strength of the GPC slab. This equation differs from that of Bradford and Pi (2013) for nonpretensioned bolted shear connectors of the type considered by Dallam (1968) and Dallam and Harpster (1968), and is a refinement of the algebraic formulations which are usually adopted for the load-slip response of conventional headed stud shear connectors reported in the literature (Olgaard et al. 1971; Johnson and Molenstra 1991; Gattesco and Giuriani 1996). A slip capacity Δ_u of at least 6 mm is considered to be sufficient to ensure ductile behavior of composite beams as suggested in Eurocode 4 [British Standards Institution (2004)]. It is worth noting that the practical design formulae proposed in this paper are applicable to HSFGB shear connectors in steel-concrete composite beams with precast GPC slabs. The compressive strength of GPC concrete is normally not less than 40 MPa.

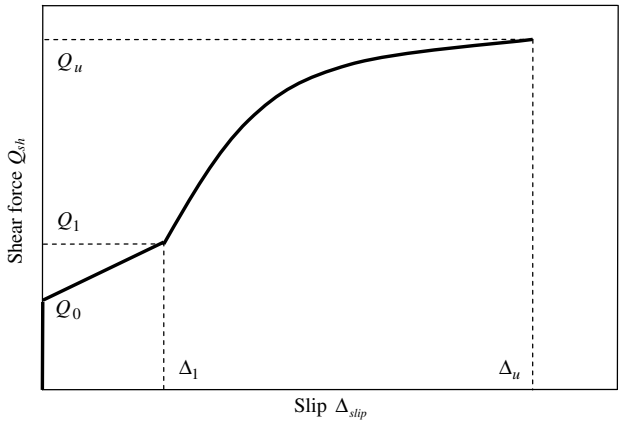

Fig. 16. Design recommendation on the load-slip relationship of HSFGB shear connector in composite beams

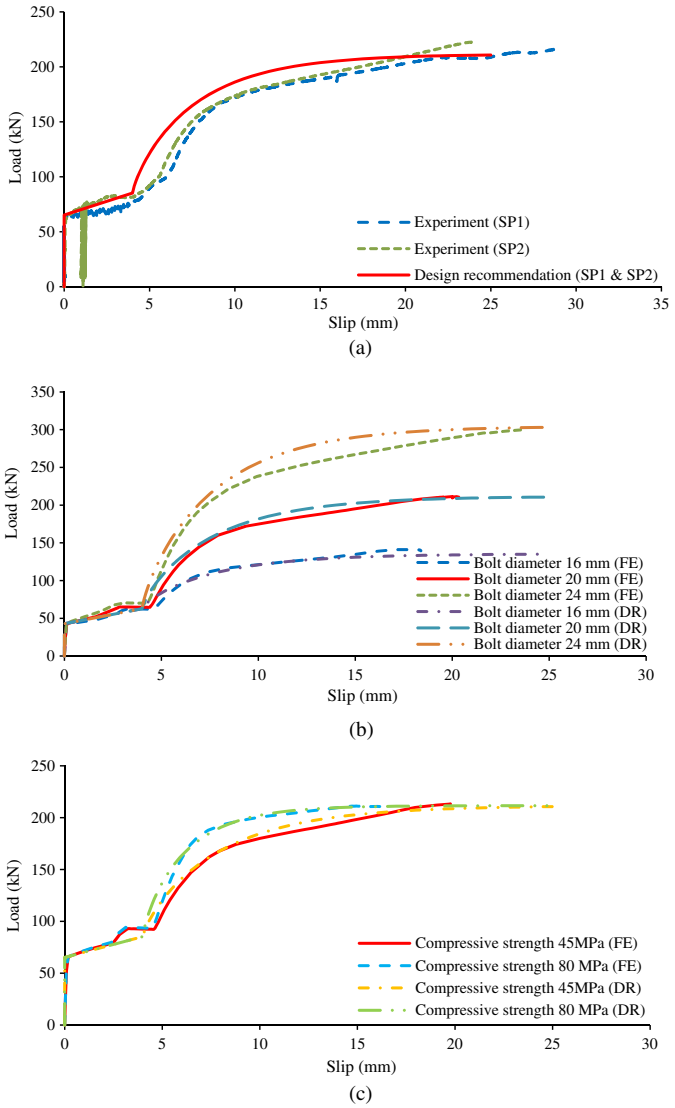

Fig. 17. Load-slip curves: (a) SP1 and SP2; (b) FE and DR for different bolt diameters; (c) FE and DR for different concrete strengths

The ultimate shear connection resistances obtained from the parametric studies have been compared with the ultimate strength of the shear connection using the proposed design recommendation. Table 3 lists comparisons of the ultimate shear connection resistances obtained from the FE analysis and the design rules proposed by Kwon et al. (2010), and the design rules suggested in the present study. The mean values of the ratios Q_{FE}/Q_{Kwon} and Q_{FE}/Q_{DR} are 1.33 and 1.01, respectively, and both with a COV of 0.011. The design rules proposed in this study are therefore able to predict the the ultimate shear resistances of HSFGB shear connectors more accurately than the proposals of Kwon et al. (2010). Fig. 17(a) shows comparisons of the load-slip curves for the specimens SP1 and SP2 obtained from the experiments and the design recommendations; Fig. 17(b) shows comparisons of the results from the FE analysis and the proposed design recommendations for specimens with different bolt diameters; and Fig. 17(c) shows comparisons of the results from the FE analysis and the proposed design recommendation for specimens with different GPC compressive strengths. Good agreement can be observed between the curves obtained from the proposed design recommendations and the results from the experiments or the FE analysis.

Conclusions

A finite element model of push-out tests has been developed to investigate the behavior of HSFGB shear connectors in composite beams with precast GPC slabs using *ABAQUS* software. This type of shear connection is proposed to expedite deconstructability within a paradigm of infrastructure sustainability. The model took into account the nonlinear material properties of the GPC, the steel beam and bolt shear connectors. Comparisons of the numerical solution with experimental results showed that the numerical model developed was capable of accurately and efficiently predicting both the ultimate strength and the load-slip curves for the shear connection. Compared with conventional headed stud shear connectors, the load-slip response of the HSFGB shear connectors exhibited three distinct regimes. At the early stage of loading, the slip almost vanished because of the pretensioned connection. After the friction at the steel-concrete interface induced by the pretension of the shear connection was overcome, significant slip took place resulting from the clearance between the prefabricated holes and the bolts. After the bolt commenced to bear against the surface of the hole in the slab, a third regime for the behavior developed. Extensive parametric studies of push-out specimens with different bolt pretensions, clearances between the holes and the bolts, diameters and tensile strengths of the bolt connectors and compressive strengths of the GPC were performed by using the numerical model. The results showed that the diameter and tensile strength of the bolt connectors had very significant effects on the ultimate shear resistances of the HSFGB shear connectors.

Practical design formulae for estimating the ultimate strengths and the load-slip relationships of shear connection achieved using HSFGB shear connectors in composite beams were also proposed, and the results compared well with the experimental and numerical results. Because these formulae are in algebraic form, they form a useful design aid for determining deflections and strengths.

Acknowledgments

The work in this paper was supported by the Australia Research Council through an Australian Laureate Fellowship (FL100100063) awarded to the second author. The assistance of the technical staff at the UNSW Heavy Structures Research Laboratory is also acknowledged with thanks.

References

ABAQUS 6.10.1 [Computer software]. Providence, RI, DassaultSystemèsSimulia.

Bradford, M. A., and Pi, Y.-L. (2012a). "Numerical modelling of deconstructable composite beams with bolted shear connectors." *Int. Conf. on Numerical Modeling Strategies for Sustainable Concrete Structures*, French Association of Civil Engineering (AFGC), Aix-en-Provence, France, 1–8.

Bradford, M. A., and Pi, Y.-L. (2012b). "Numerical modelling of composite steel-concrete beams for life cycle deconstructability." *1st Int. Conf. on Performance-Based and Life-Cycle Structural Engineering*, Hong Kong Polytechnic Univ., Hong Kong.

Bradford, M. A., and Pi, Y.-L. (2013). "Nonlinear elastic-plastic analysis of composite members of high-strength steel and geopolymer concrete." *Comput. Model. Eng. Sci.*, 89(5), 387–414.

British Standards Institution. (2004). "Eurocode 4: Design of composite steel and concrete structures—Part 1.1: General rules and rules for building." *EN 1994-1-1*, London.

Collins, M. P., Mitchell, D., and MacGregor, J. G. (1993). "Structural design considerations for high strength concrete." *Concr. Int.*, 15(5), 27–34.

Dallam, L. N. (1968). "Pushout tests with high strength bolt shear connectors." *Rep. 68-7*, Dept. of Civil Engineering, Univ. of Missouri-Columbia, Columbia, MO.
Dallam, L. N., and Harpster, J. L. (1968). "Composite beams tests with high-strength bolt shear connectors." *Rep. 68-3*, Dept. of Civil Engineering, Univ. of Missouri-Columbia, Columbia, MO.
Davidovits, J., Comrie, D. C., Paterson, J. H., and Ritcey, D. J. (1990). "Geopolymeric concrete for environmental protection." *Concr. Int.*, 12(7), 30–39.
Ellobody, E., and Lam, D. (2002). "Modelling of headed stud in steel-precast composite beams." *Steel Compos. Struct.*, 2(5), 355–378.
Gattesco, N., and Giuriani, E. (1996). "Experiemental study on stud shear connectors subjected to cycling loading." *J. Constr. Steel Res.*, 38(1), 1–21.
Hardjito, D., and Rangan, B. V. (2005). "Development and properties of low calcium fly ashbased geopolymer concrete." *Research Rep. GC1*, Curtin Univ. of Technology, Perth, WA, Australia.
Institution of Structural Engineers. (2012). ⟨http://cic.org.uk/admin/resources/the-institution-of-structural-engineers-.pdf⟩ (Sep. 1, 2013).
Johnson, R. P. (2004). *Composite structures of steel and concrete: Beams, slabs, columns, and frames for buildings*, Blackwell Publishing, Oxford, U.K.
Johnson, R. P., and Molenstra, N. (1991). "Partial connection in composite beams for buildings." *Proc., ICE*, 91(4), 679–704.
Kwon, G., Engelhardt, M. D., and Klingner, R. E. (2010). "Behavior of post-installed shear connectors under static and fatigue loading." *J. Constr. Steel Res.*, 66(4), 532–541.
Lam, D., and Ellobody, E. (2005). "Behavior of headed stud shear connectors in composite beams." *J. Struct. Eng.*, 10.1061/(ASCE)0733-9445(2005)131:1(96), 96–107.
Lee, S. S. M., and Bradford, M. A. (2013a). "Sustainable composite beam behaviour with deconstructable bolted shear connectors." *Compos. Constr. VII*, Centre for Infrastructure Engineering and Safety at the Univ. of New South Wales, Sydney, Australia.
Lee, S. S. M., and Bradford, M. A. (2013b). "Sustainable composite beams with deconstructable bolted shear connectors." *5th Int. Conf. on Structural Engineering, Mechanics and Computation*, Taylor & Francis Group, London.
Loh, H. Y., Uy, B., and Bradford, M. A. (2006). "The effects of partial shear connection in composite flush end plate joints. Part I—Experimental study." *J. Constr. Steel Res.*, 62(4), 378–390.
Marshall, W. T., Nelson, H. M., and Banerjee, H. K. (1971). "An experimental study of the use of high-strength friction-grip bolts as shear connectors in composite beams." *Struct. Eng.*, 49(4), 171–178.
McCaffrey, R. (2002). "Climate change and the cement industry." *Global Cem. Lime Mag.* (Environmental Special Issue), 15–19.
National Sustainability Council. (2013). ⟨http://www.environment.gov.au/sustainability/measuring/council.html⟩ (Sep. 1, 2013), Australian Government, Canberra, Australia.
Ng, T. S., and Foster, S. J. (2008). "Development of high performance geopolymer concrete." *20th Australasian Conf. on the Mechanics of Structures and Materials*, Univ. of Southern Queensland, Toowoomba, QLD, Australia, 329–335.
Nguyen, H. T., and Kim, S. E. (2009). "Finite element modeling of push-out tests for large stud shear connectors." *J. Constr. Steel Res.*, 65(10), 1909–1920.
Oehlers, D. J., and Bradford, M. A. (1995). *Composite steel and concrete structural members: Fundamental behavior*, Pergamon, Oxford, U.K.
Olgaard, J. G., Slutter, R. G., and Fisher, J. W. (1971). "Shear strength of stud connectors in lightweight and normal weight concrete." *AISC Eng. J.*, 8(2), 55–64.
Pavlovic, M., Spremic, M., Markovic, Z., and Veljkovic, M. (2013). "Headed shear studs versus high-strength bolts in prefabricated composite decks." *Compos. Construct. VII*, Centre for Infrastructure Engineering and Safety at the Univ. of New South Wales, Sydney, Australia.
Rangan, B. V. (2009). "Engineering properties of geopolymer concrete." Chapter 13, *Geopolymers: Structures, processing, properties and applications*, J. L. Provis and J. S. V. van Deventer, eds., Woodhead Publishing, London.
Shi, G., Shi, Y., Wang, Y., and Bradford, M. A. (2008). "Numerical simulation of steel pretensioned bolted end-plate connections of different types and details." *Eng. Struct.*, 30(10), 2677–2686.
Standards Australia. (1996). *AS3679 Structural steel—Part 1: Hot-rolled bars and sections*, Sydney, Australia.
Standards Australia. (1997). *AS1012 Methods of testing concrete—Part 17: Determination of the static chord modulus of elasticity and Poisson's ratio of concrete specimens*, Sydney, Australia.
Standards Australia. (1998). *AS4100 Steel structures*, Sydney, Australia.
Standards Australia. (1999). *AS1012 Methods of testing concrete—Part 9: Determination of the compressive strength of concrete specimens*, Sydney, Australia.
Standards Australia. (2009). *AS3600 Concrete structures*, Sydney, Australia.
Trahair, N. S., Bradford, M. A., Nethercot, D. A., and Gardner, L. (2008). *The behaviour and design of steel structures to EC3*, Taylor-Francis, London.
Vanegas, J. A., ed. (2004). *Sustainable engineering practice: An introduction*, ASCE, Reston, VA.
Viest, I. M., Colaco, J. P., Furlong, R. W., Griffis, L. G., Leon, R. T., and Wyllie, L. A., Jr. (1997). *Composite construction design for buildings*, Mc-Graw Hill, New York.